

GSA Data Repository 2018218

*Ongoing transient bedrock incision of the Forty Mile River driven by Late Pliocene Yukon River capture,
eastern Alaska and Yukon, Canada*

Adrian Bender¹, Richard Lease¹, Lee Corbett², Paul Bierman² and Marc W. Caffee³

¹U.S. Geological Survey Alaska Science Center, Anchorage, Alaska, 99508; email: abender@usgs.gov

²University of Vermont, Department of Geology, Burlington, VT 05405

³Department of Physics and Astronomy, and Department of Earth, Atmospheric, and Planetary Sciences
Purdue University, 525 Northwestern Avenue, West Lafayette, IN 47907

EXPANDED METHODS

Disclaimer

Any use of trade, firm, or product names is for descriptive purposes only and does not imply endorsement by the U.S. Government.

Cosmogenic isochron burial dating

The isochron method (Balco and Rovey, 2008) generally requires sampling quartz-bearing material spanning a range of pre-burial isotope concentrations from a single horizon (indicative of common burial history) buried by several m of sediment (sufficient to minimize post-burial production). We satisfy these sampling requirements at a shallow pit (sample horizon from 3.2–3.5 m depth) in the Forty Mile River terrace gravel at a site we refer to as Clinton Creek located ~7 km upstream of the Forty Mile–Yukon River confluence (Fig. DR1). The isochron method involves fitting a line to measured nuclide concentrations and analytical uncertainties, with ^{10}Be and ^{26}Al on the x- and y-axes, respectively (e.g., Bender et al., 2016). We use the York regression method housed in Isoplot 4.15 (<http://www.bgc.org/isoplot/etc/isoplot.html>) that considers x and y uncertainties (e.g., Mahon, 1996). The slope (R_{meas}) of the line fit to the measured concentrations reflects the deviation from the surface ^{26}Al : ^{10}Be production ratio (R_{init} ; Fig. DR2). The slope deviation depends on isotope half-life and duration of post-burial decay, so the burial age (t_b) is calculated as:

$$t_b = -\ln(R_{\text{meas}}/R_{\text{init}})/(\lambda_{26} - \lambda_{10}) \quad (1)$$

In keeping with other published applications of the isochron method (c.f. Schaller et al., 2016) we use the commonly accepted but poorly empirically constrained R_{init} value of 6.75 (e.g., Corbett et al., 2017). Decay constants λ_{26} ($9.83 \pm 0.25 \times 10^{-7}/\text{yr}$) and λ_{10} ($5.00 \pm 0.26 \times 10^{-7}/\text{yr}$) equate with half-lives of 0.705 Myr for ^{26}Al (Nishiizumi, 2004) and 1.387 Myr for ^{10}Be (c.f., Chmeleff et al., 2010).

A key goal for the Forty Mile River terrace gravel age is comparison and correlation with the Cordilleran Ice Sheet (CIS)-related gravel dated by Hidy and others (2013, 2018) between $1.12^{+0.44/-0.36}$ and $2.84^{+0.22/-0.19}$ Ma. Comparing these ages requires parallel comparison of the respective methods, and the processes being dated. We use the same laboratory standards and decay constants assumed in the ^{26}Al - ^{10}Be ages of Hidy and others (2013, 2018), but our sampling and computational approaches differ. Whereas we use the isochron approach (Balco and Rovey, 2008), Hidy and others (2013, 2018) calculate (a) a $2.84^{+0.22/-0.19}$ Ma simple depositional age based on burial plot analysis of clasts from different depths across the CIS-over-local gravel contact, and (b) a $1.12^{+0.44/-0.36}$ Ma depth profile exposure age of soil developed at the terrace surface of the CIS gravel. These ages bracket the onset of CIS terrace gravel deposition (~2.84 Ma) and the stabilization of the terrace surface (~1.12 Ma) such that a depositional age of terrace gravel that falls within this range correlates temporally to aggradation-prone sediment flux and discharge conditions imposed by the CIS climate (e.g., Hancock and Anderson, 2002). Moreover, Hidy and others (2018) interpret lower-than-expected in-situ isotope ratios in their exposure age depth profile as the result of isotope production impeded by temporally intermittent loess cover. We note that because the isochron technique relies on the pre-burial isotope inheritance of each sample, and not in situ-produced concentrations analyzed by depth profile techniques, the depositional age we compute (via the isochron technique) is not sensitive to intermittent burial by loess or other deposits.

^{10}Be -based tributary erosion rates

We quantify basin-averaged erosion rates using ^{10}Be concentrations measured in quartz from modern river sand (250–850 μm) at six tributary outlets on the Forty Mile River. ^{10}Be accumulates in quartz at Earth's surface to depths commensurate with cosmic ray e-folding length (~0.6 m in rock), at rates determined largely by latitude and altitude (e.g., Lal, 1991; Stone, 2000) and inversely proportional to erosion rate (e.g., Brown et al., 1995; Granger et al., 1996; Bierman and Steig, 1996). Dividing the ^{10}Be

production depth by a given measured erosion rate thus estimates the duration of erosion at the measured rate. Given similar rock type and durability throughout the Fortymile River basin and minimal lithologic variation within the sampled tributary catchments (Foster, 1976), we make the simple assumption that quartz sampled at the 250-850 μm grain size range is well-mixed and represents erosion throughout the tributary catchment upstream. We calculate the ^{10}Be production rate-weighted average elevation and latitude for each sample catchment (e.g., Brown et al., 1995; Granger et al., 1996; Bierman and Steig, 1996; Portenga and Bierman, 2011), and use the CRONUS online calculator (<https://hess.ess.washington.edu/>) to assess erosion rates based on ^{10}Be concentrations at each outlet (Balco et al., 2008). Topographic shielding minimally impacts ^{10}Be production rates because topography is relatively open in the basins we sample, with average hillslopes of 6° to 16° (e.g., Bierman and Steig, 1996). Similarly, the mean winter snow depth of <50 cm measured at Fortymile Basin SNOTEL sites 1275 and 1189 (<https://wcc.sc.egov.usda.gov/nwcc/>) confers shielding effects that contribute ~1-3% uncertainty by some estimates (Gosse and Phillips, 2001). Schildgen and others (2005) show that, in certain locations, snow cover can reduce the long-term (15.5 ka) ^{10}Be production rate up to 14%, and suggest that using contemporary climate data to estimate snow shielding may inject systematic error into ^{10}Be production assessment and derivative calculations. Instead of attempting to explicitly treat snow or topographic shielding effects, we subsume the expected minimal snow and topographic shielding effects on ^{10}Be production rate by directly adding 5% of each CRONUS-reported rate to the attendant reported uncertainty.

Bedrock incision

We infer bedrock incision rates by dividing strath height over the terrace gravel age (~2.44 Ma). We compute strath height as the difference between channel elevation, gravel thickness (tread to strath), and terrace tread (gravel top) elevation. We measured terrace gravel thickness (range 5 to 25 m) using a laser range finder or tape measure at four sites along the studied river reach, among which we observe linear upstream thinning ($y = -0.11x + 24$ where y represents gravel thickness in meters and x represents river distance in kilometers; $R^2 = 0.95$) that we use to extrapolate gravel thickness along the river. We use the active channel as a vertical datum for incision given that (a) the active channel occupies an elevation between the bedrock channel bed and flood stage levels at which lateral and vertical incision likely occur (e.g., Lague, 2014), (b) the ~2.44 Ma time interval over which we average bedrock incision approaches the upper limit of the time range over which bedrock incision rates may decrease as a function of age (Finnegan et al., 2014; Gallen et al., 2015), and (c) our channel profile analysis indicates that the entire knickzone remains in a transient state wherein active channel adjustment via bedrock incision likely continues to the present. Finally, we acknowledge that using a single terrace gravel age to infer rates of incision implicitly neglects the probable upstream decrease in gravel age that should reflect progressive terrace abandonment downstream of a headward-propagating knickzone, and therefore consider as minima the incision rates thusly inferred.

Stream power model

We analyze the Fortymile River longitudinal profile using the relationship between dimensionless channel slope (S) and drainage area (A , m^2) observed among equilibrium-state channels (e.g., Sklar and Dietrich, 1998):

$$S = k_s A^{-\theta} \quad (2)$$

Indices of channel steepness (k_s) and concavity (θ) represent the y-intercept and slope of a logarithmic regression of A and S , respectively. Fixing θ at a reference value (θ_{ref}) allows assessment of a channel steepness index normalized to drainage area (k_{sn}) (Wobus et al., 2006), permitting quantitative comparison of geometrically distinct river reaches:

$$S = k_{sn} A^{-\theta_{ref}} \quad (3)$$

We use knickzone incision rates to calibrate and test a common stream power incision model (e.g., Whipple and Tucker, 1999) that approximates bedrock incision rate (I , m/y) as a power law function of A and S:

$$I = KA^mS^n \quad (4)$$

Positive constants m and n reflect channel morphology, and K represents a dimensional coefficient of erosion (units of m^{1-2m}) (e.g., Whipple and Tucker, 1999). The solution for S implicit in (4) takes the form of (3), assuming constant downstream K and n , such that k_{sn} and θ_{ref} equal the stream power terms $(I/K)^{1/n}$ and m/n , respectively. We use the term compatibility between (3) and (4) to calculate K , m , and n based on headwaters k_{sn} value of 228 and $m/n = \theta_{ref} = 0.6 \sim \theta_{\text{headwaters}}$ (the high end of model-predicted m/n values, 0.35 to 0.6; Whipple and Tucker, 1999).

We infer I from terrace tread elevation, gravel thickness, active channel elevation and the terrace gravel age averaged on 10 km river distance bins along the Fortymile River knickzone, and use the bin-averaged incision rates to solve for K linearly proportional to basal shear stress ($n = 2/3$ and therefore $m = 2/5$) and stream power ($n = 1$ and therefore $m = 3/5$). To discern a suitable, constant value of K , we iteratively test values of K within the range published by Stock and Montgomery (1999) in an initial coarse search, and tighten the search interval for a fine search at the order of magnitude scale. We rearrange equation (4) to solve for knickzone channel elevation by treating S as the downstream change in elevation over distance, and systematically model the knickzone reach of the Fortymile River long profile for K values within the apparent order of magnitude that the suitable value of K resides. We converge on a suitable K value by minimizing the difference between regression equations from linear fits of the 10 km distance-binned modeled channel elevations against distance (for cases where bedrock incision is linearly proportional to shear stress and stream power) and the linear elevation-distance relationship computed for the knickzone ($y = 1.621x + 267.5$). We calculate absolute differences in regression statistics and collect and plot each against the corresponding value of K , fitting lines that slope positively and negatively toward x-intercepts that bracket the best value of K . We use the linear fits (Fig. DR3) to calculate four values of K for both the stream power and shear stress cases, and average the values (which generally vary at the second or third decimal place) to ascertain a single uniform K value for each case.

TABLES

Table DR1: ^{10}Be data

Table DR2: ^{26}Al data

Table DR3: Basin-average erosion rate data submitted to CRONUS

Table DR4: Basin-average erosion rate output from CRONUS

Table DR5: ^{10}Be and ^{26}Al blank ratios

FIGURES

Figure DR1: Description for isochron burial age sample site 16ALR247 (Clinton Creek).

Figure DR2: Isochron plot with Clinton Creek data and line representing surface production ratio.

Figure DR3: Minimization plots used to quantify uniform Fortymile River K values.

Table DR1: ^{10}Be data

Analysis	Site	latitude	longitude*	DEM elevation (m)**			sample	sub-sample	sample type***	material type	Quartz Mass (g)	Mass of ^{10}Be Added (ug)****	AMS Cathode Number	Measured $^{10}\text{Be}/\text{Be}$ Ratio*****	Measured $^{10}\text{Be}/\text{Be}$ Ratio uncertainty*****	Background-Corrected $^{10}\text{Be}/\text{Be}$ Ratio	Background-Corrected $^{10}\text{Be}/\text{Be}$ Ratio uncertainty	^{10}Be Concentration (atoms/g)	^{10}Be Concentration Uncertainty (atoms/g)
				1	c	quartz													
isochron buri al age	Clinton Creek	64.37448	-140.59348	566	16ALR247	1	c	quartz	21.0	241.0	144600	2.65E-13	8.10E-15	2.64E-13	8.12E-15	2.02E+05	6.22E+03		
						2	c	quartz	20.9	240.3	144602	1.85E-13	6.65E-15	1.84E-13	6.67E-15	1.42E+05	5.13E+03		
						7	c	quartz	20.5	240.8	144603	4.10E-13	1.00E-14	4.09E-13	1.00E-14	3.21E+05	7.87E+03		
						9	c	quartz	21.7	241.5	144604	2.76E-13	8.25E-15	2.75E-13	8.27E-15	2.05E+05	6.15E+03		
						16A	p	mix	21.8	241.3	144605	2.92E-13	8.21E-15	2.91E-13	8.23E-15	2.02E+05	6.20E+03		
						16B	s	mix	21.4	241.7	144606	3.16E-13	8.21E-15	3.15E-13	8.23E-15	2.37E+05	6.20E+03		
	Sam Patch	64.31638	-141.00849	331	16ALR216	--	rs	mix	18.0	242.0	142742	3.61E-13	1.01E-14	3.60E-13	1.01E-14	3.24E+05	9.11E+03		
	Jet Boat	64.25529	-141.72489	438	16ALR220	--	rs	mix	11.6	241.1	142743	2.81E-13	7.28E-15	2.80E-13	7.28E-15	3.88E+05	1.01E+04		
	Big Burn	63.90196	-142.12326	548	16ALR225	--	rs	mix	20.0	241.0	142744	4.33E-13	9.04E-15	4.32E-13	9.05E-15	3.47E+05	7.28E+03		
	Bear Paw	63.79564	-142.52548	622	16ALR227	--	rs	mix	13.8	240.9	142746	5.26E-13	1.05E-14	5.25E-13	1.06E-14	6.15E+05	1.24E+04		
erosion rate	Tussock	63.60166	-142.75092	676	16ALR228	--	rs	mix	19.7	241.5	142747	7.40E-13	1.37E-14	7.39E-13	1.37E-14	6.04E+05	1.12E+04		
	Maiden Ck	64.38262	-140.62373	315	16ALR246	--	rs	mix	15.5	241.1	142748	2.81E-13	7.62E-15	2.80E-13	7.64E-15	2.92E+05	7.95E+03		
	Wall Street Ck	64.05824	-141.76432	481	16ALR248	--	rs	mix	11.2	240.8	142749	3.01E-13	1.02E-14	3.00E-13	1.02E-14	4.32E+05	1.47E+04		

^{10}Be samples were processed in three batches containing two blanks each. Blanks (n=6) have an average $^{10}\text{Be}/\text{Be}$ ratio of 8.49E-16 ± 5.45E-16 (Table DR5). Uncertainty in blanks was added quadratically. Quoted uncertainties represent the 1 σ range.

*Projection: NAD_1983 Alaska_Albers

**Elevation from the National Elevation Database Alaska DEM, available by searching <https://viewer.nationalmap.gov/basic/>

***c = clast, p = amalgamated matrix pebbles, s = amalgamated matrix sand

****Be was added through a beryl carrier made at University of Vermont.

*****Isotopic analysis was conducted at PRIME Laboratory; ratios were normalized against standard 07KNSTD3110 with an assumed ratio of 2850 × 10⁻¹⁵ (Nishizumi et al., 2007).

Table DR2: ^{26}Al data

Analysis	Site	latitude*	longitude*	DEM elevation (m)**			sample	sub-sample	sample type***	material type	Quartz Mass (g)	Total ^{27}Al Quantified by ICP-OES (ug)****	AMS Cathode Number	Measured $^{26}\text{Al}/^{27}\text{Al}$ Ratio*****	Measured $^{26}\text{Al}/^{27}\text{Al}$ Ratio uncertainty*****	Background-Corrected $^{26}\text{Al}/^{27}\text{Al}$ Ratio	$^{26}\text{Al}/^{27}\text{Al}$ Ratio uncertainty	^{26}Al Concentration (atoms/g)	^{26}Al Concentration Uncertainty (atoms/g)
				1	c	quartz													
isochron buri al age	Clinton Creek	64.37448	-140.59348	566	16ALR247	1	c	quartz	21.0	1446	144600	5.76E-13	2.93E-14	5.75E-13	2.93E-14	8.83E+05	4.49E+04		
						2	c	quartz	20.9	1481	144632	4.13E-13	1.56E-14	4.12E-13	1.56E-14	6.52E+05	2.47E+04		
						7	c	quartz	20.5	1749	144633	5.26E-13	2.15E-14	5.25E-13	2.15E-14	1.00E+06	4.10E+04		
						9	c	quartz	21.7	1486	144634	5.30E-13	1.94E-14	5.30E-13	1.94E-14	8.09E+05	2.97E+04		
						16A	p	mix	21.8	1571	144635	4.82E-13	1.72E-14	4.81E-13	1.72E-14	7.76E+05	2.77E+04		
						16B	s	mix	21.4	2604	144636	3.44E-13	1.28E-14	3.43E-13	1.28E-14	9.31E+05	3.48E+04		

^{26}Al samples were processed in two batches along with a total of five blanks. Blanks (n=5) have an average $^{26}\text{Al}/^{27}\text{Al}$ ratio of 7.67E-16 ± 4.68E-16 (Table DR5). Uncertainty in blanks was added quadratically. Quoted uncertainties represent the 1 σ range.

*Projection: NAD_1983 Alaska_Albers

**Elevation from the National Elevation Database Alaska DEM, available by searching <https://viewer.nationalmap.gov/basic/>

***c = clast, p = amalgamated matrix pebbles, s = amalgamated matrix sand

****Al was added only to samples with insufficient total Al through commercial SPEX ICP standard with a concentration of 1000 µg mL⁻¹. The total here reflects the sum of Al added through carrier and native Al in quartz.

*****Isotopic analysis was conducted at PRIME Laboratory; ratios were normalized against standard KNSTD with an assumed ratio of 1.818 × 10⁻¹² (Nishizumi et al., 2004).

Table DR3: Basin-average erosion rate data submitted to CRONUS

Sample name	Latitude	Longitude	Elevation (m)	Elevation flag	Sample thickness (cm)	Sample density (g/cm ³)	Shielding correction	^{10}Be concentration (atoms/g)*	Uncertainty in ^{10}Be concentration (atoms/g)**		Name of Be-10 standardization	Uncertainty in ^{26}Al concentration (atoms/g)**		Name of Al-26 standardization
									standardization	concentration		standardization	concentration	
ALR216	64.37094	-141.05040	769	std	1	2.7	1	3.24E+05	9.11E+03	0	0	0	0	KNSTD
ALR220	64.22979	-141.63644	831	std	1	2.7	1	3.88E+05	1.01E+04	0	0	0	0	KNSTD
ALR225	63.84553	-142.10678	838	std	1	2.7	1	3.47E+05	7.28E+03	0	0	0	0	KNSTD
ALR227	63.81671	-142.54467	818	std	1	2.7	1	6.15E+05	1.24E+04	0	0	0	0	KNSTD
ALR228	63.82325	-142.81789	700	std	1	2.7	1	6.04E+05	1.12E+04	0	0	0	0	KNSTD
ALR246	64.37084	-140.58320	543	std	1	2.7	1	2.92E+05	7.95E+03	0	0	0	0	KNSTD
ALR248	64.04259	-141.70429	819	std	1	2.7	1	4.32E+05	1.47E+04	0	0	0	0	KNSTD

*production rate weighted (e.g., Portenga and Bierman, 2011)

**Quoted uncertainties represent the 1 σ range.

Table DR4: Basin-average erosion rate results from CRONUS*

Sample name	Shielding factor	Production rate (muons/yr) (atoms/g/yr)	Internal uncertainty (m/Myr)	Erosion rate ((g/cm ³)/yr)	Erosion rate (m/Myr)	External uncertainty (m/Myr)	Production rate (spallation) (atoms/g/yr)
ALR216	1	0.10	0.52	4.81E-03	17.82	1.51	8.97
ALR220	1	0.10	0.42	4.20E-03	15.54	1.32	9.49
ALR225	1	0.10	0.38	4.74E-03	17.57	1.46	9.55
ALR227	1	0.10	0.20	2.56E-03	9.47	0.81	9.37
ALR228	1	0.10	0.17	2.34E-03	8.68	0.74	8.42
ALR246	1	0.09	0.46	4.38E-03	16.23	1.36	7.26
ALR248	1	0.10	0.49	3.71E-03	13.76	1.21	9.38

*Calculated May 6, 2018 at <https://hess.eos.washington.edu> using wrapper script v2.3, main calculator v2.1, objective function v2.0, constants v2.3, muons v1.1 and the Lal(1991)/Stone(2000) global production rate scaling scheme for spallation.

**Below Detection Limit

Table DR5: ^{10}Be and ^{26}Al blank ratios*

^{10}Be	^{26}Al
Blank Name	UVM Batch Number
BLK	607
BLK	607
BLK	608
BLK	608
BLK	613
BLK	609
BLK	607
BLK	608
BLK	613
BLK	613
BLK	609
BLK	607
BLK	608
BLK	609
BLK	607
BLK	608
BLK	609
BLK	607
BLK	608
BLK	609
BLK	607
BLK	608
BLK	609

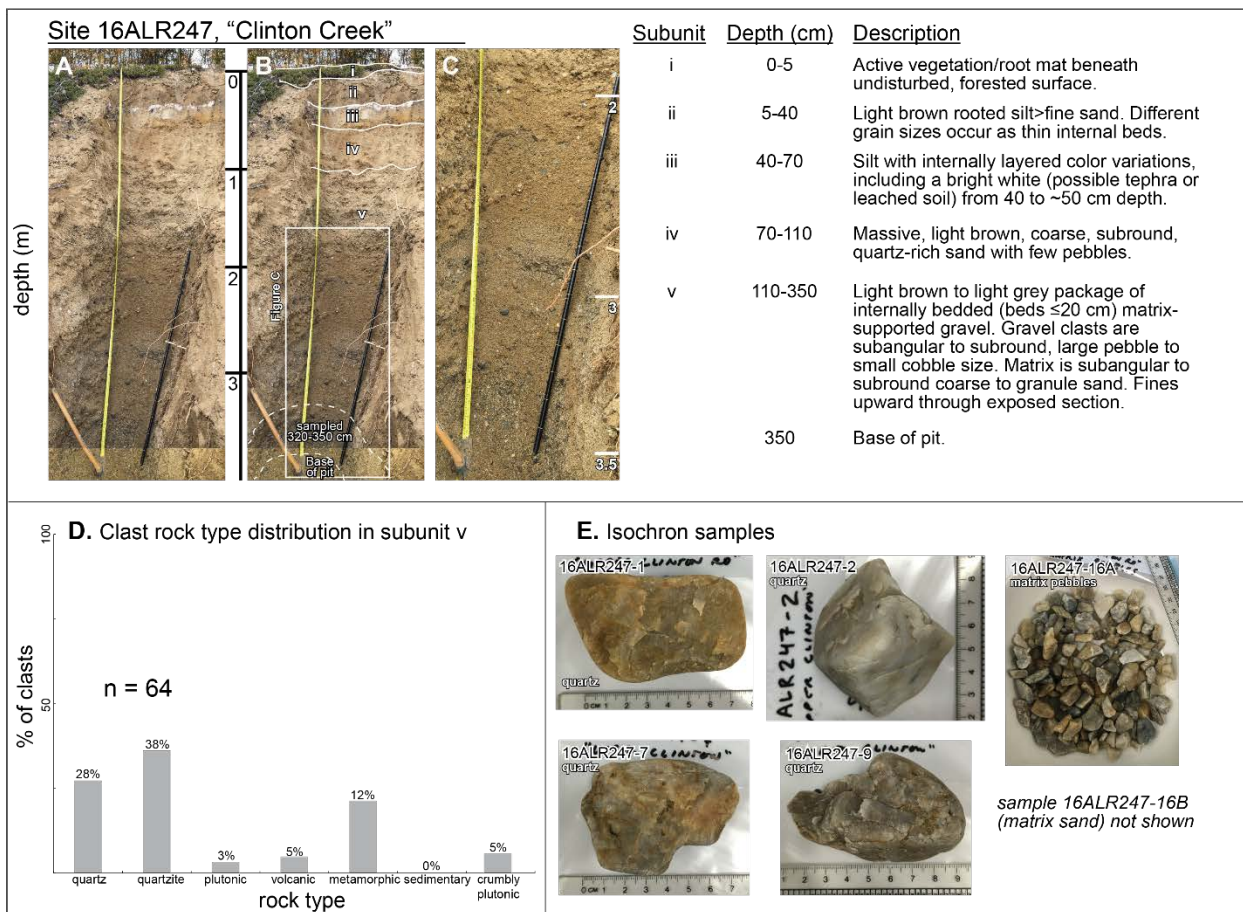


Figure DR1: Description for isochron burial age sample site 16ALR247, located in Yukon, Canada near the Forty-mile-Yukon River confluence at NAD1983 UTM coordinates 64.37448, -140.59348. (A) Uninterpreted photo of sample pit. (B) Sample pit with stratigraphic interpretation of subunits. Solid white lines represent contacts, dashed white lines represent sampled interval, from 320 cm to the base of the pit at 350 cm. (C) Enlarged, un-interpreted photo of subunit v, which we sampled the bottom 30 cm of for cosmogenic isochron burial dating. (D) Rock type percentages from a count of 64 clasts in subunit v (110-350 cm depth). (E) Samples submitted for cosmogenic isochron burial age analysis (Tables DR1, DR2). Rock type for cobbles indicated in white text. Scale is shown in centimeters and varies between photos. Amalgamated matrix pebbles and sand (not shown) processed and treated as individual samples.

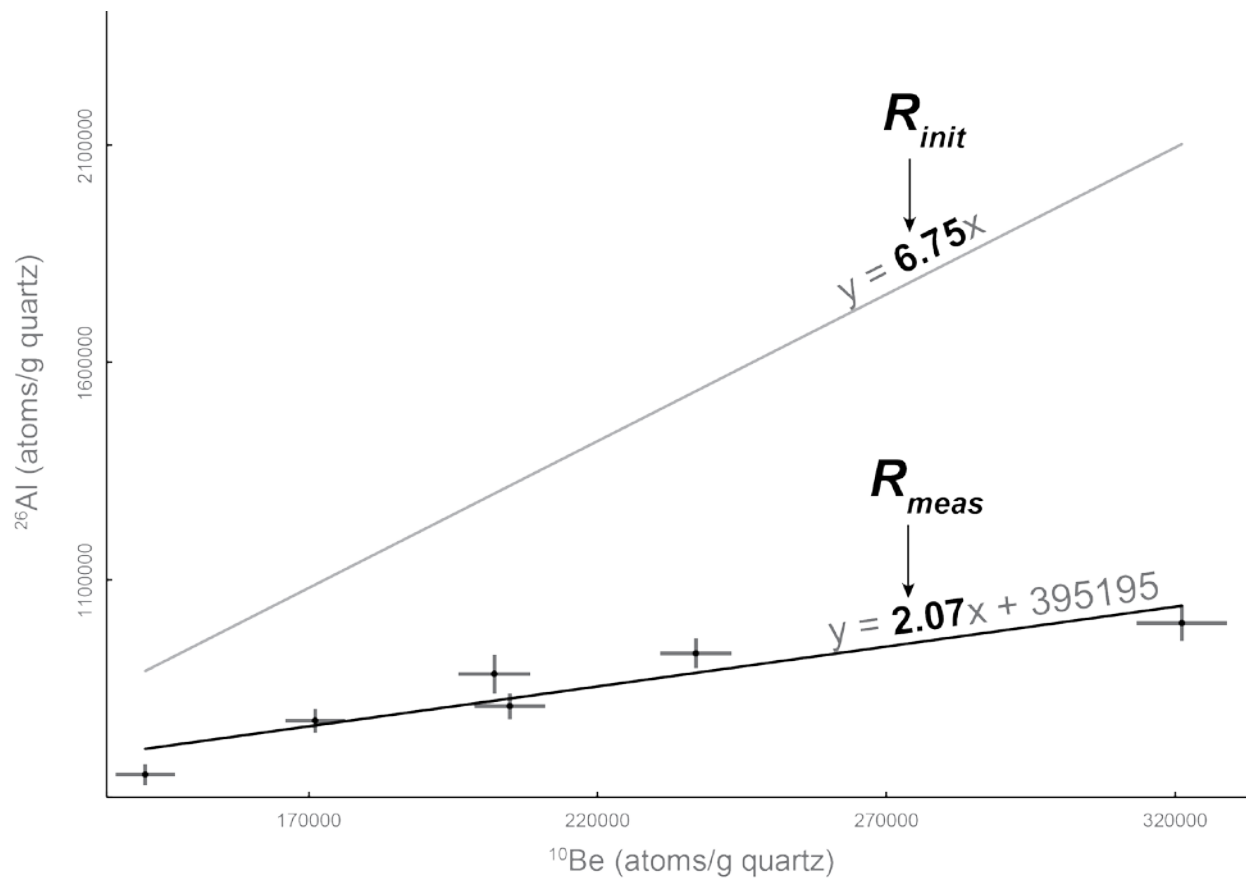


Figure DR2: Isochron plot with line fit to Clinton Creek data (slope provides R_{meas}) and line representing surface production ratio for the Clinton Creek samples (R_{init} assumed ~6.75).

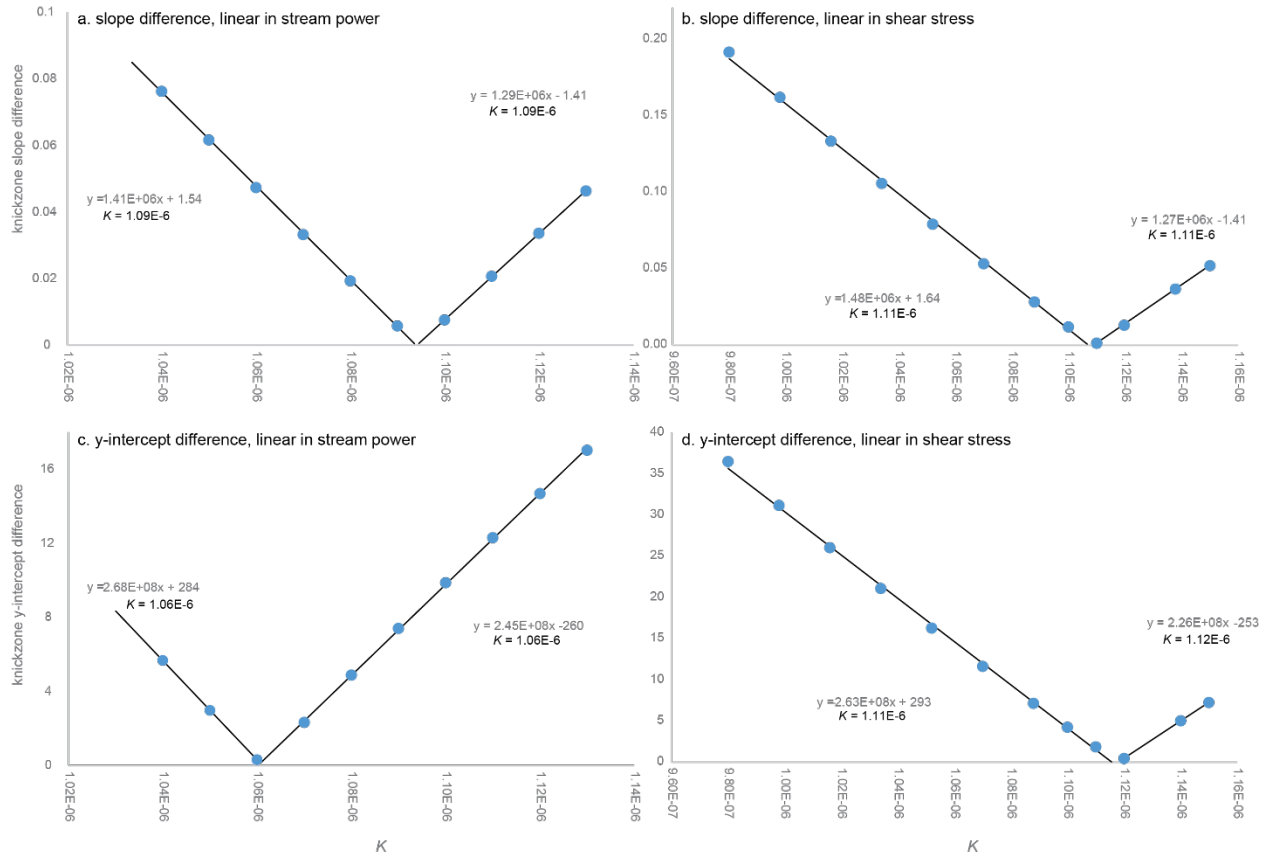


Figure DR3: Plots used to quantify a uniform Forty-mile River K value from minimized linear regression statistic differences. (A) Difference in slope from modeled and DEM knickzone long profiles plotted over K value where $m = 0.6$ and $n = 1$ such that bedrock incision is linearly proportional to stream power, and (B) where $m = 0.4$ and $n = 0.67$ such that bedrock incision is linearly proportional to shear stress. (C) Difference in y-intercept from regressions of modeled and DEM knickzone long profiles plotted over K value where $m = 0.6$ and $n = 1$ such that bedrock incision is linearly proportional to stream power, and (D) where $m = 0.4$ and $n = 0.67$ such that bedrock incision is linearly proportional to shear stress.

REFERENCES CITED

- Balco, G. and Rovey, C.W., 2008. An isochron method for cosmogenic-nuclide dating of buried soils and sediments. *American Journal of Science*, 308(10), pp.1083-1114.
- Bender, A.M., Amos, C.B., Bierman, P., Rood, D.H., Staisch, L., Kelsey, H. and Sherrod, B., 2016. Differential uplift and incision of the Yakima River terraces, central Washington State. *Journal of Geophysical Research: Solid Earth*, 121(1), pp.365-384.
- Bierman, P. and Steig, E.J., 1996. Estimating rates of denudation using cosmogenic isotope abundances in sediment. *Earth surface processes and landforms*, 21(2), pp.125-139.
- Brown, E.T., Stallard, R.F., Larsen, M.C., Raisbeck, G.M., Yiou, F., 1995. Denudation rates determined from the accumulation of in situ-produced ^{10}Be in the Luquillo experimental forest, Puerto Rico, *Earth and Planetary Science Letters*, v. 129, p.193-202, ISSN 0012-821X.
- Chmeleff, J., von Blanckenburg, F., Kossert, K. and Jakob, D., 2010. Determination of the ^{10}Be half-life by multicollector ICP-MS and liquid scintillation counting. *Nuclear Instruments and Methods in Physics Research Section B: Beam Interactions with Materials and Atoms*, 268(2), pp.192-199.
- Corbett, L.B., Bierman, P.R., Rood, D.H., Caffee, M.W., Lifton, N.A. and Woodruff, T.E., 2017. Cosmogenic $^{26}\text{Al}/^{10}\text{Be}$ surface production ratio in Greenland. *Geophysical Research Letters*, 44(3), pp.1350-1359.
- Foster, H.L., 1976, Geologic map of the Eagle quadrangle, Alaska: U.S. Geological Survey Miscellaneous Investigations Series Map 1-922, scale 1:250,000.
- Finnegan, N.J., Schumer, R. and Finnegan, S., 2014. A signature of transience in bedrock river incision rates over timescales of 10^4 - 10^7 years. *Nature*, 505(7483), p.391.
- Gallen, S.F., Pazzaglia, F.J., Wegmann, K.W., Pederson, J.L. and Gardner, T.W., 2015. The dynamic reference frame of rivers and apparent transience in incision rates. *Geology*, 43(7), pp.623-626.
- Gosse, J.C. and Phillips, F.M., 2001. Terrestrial in situ cosmogenic nuclides: theory and application. *Quaternary Science Reviews*, 20(14), pp.1475-1560.
- Granger, D.E., Kirchner, J.W. and Finkel, R., 1996. Spatially averaged long-term erosion rates measured from in situ-produced cosmogenic nuclides in alluvial sediment. *The Journal of Geology*, 104(3), pp.249-257.
- Hancock, G.S. and Anderson, R.S., 2002. Numerical modeling of fluvial strath-terrace formation in response to oscillating climate. *Geological Society of America Bulletin*, 114(9), pp.1131-1142.
- Hidy, A.J., Gosse, J.C., Froese, D.G., Bond, J.D. and Rood, D.H., 2013. A latest Pliocene age for the earliest and most extensive Cordilleran Ice Sheet in northwestern Canada. *Quaternary Science Reviews*, 61, pp.77-84.
- Hidy, A.J., Gosse, J. C., Sanborn, P., Froese, D. G., 2018. Age-erosion constraints on an Early Pleistocene paleosol in Yukon, Canada, with profiles of ^{10}Be and ^{26}Al : Evidence for a significant loess cover effect on cosmogenic nuclide production rates, *CATENA*, v. 165, p. 260-271, ISSN 0341-8162, <https://doi.org/10.1016/j.catena.2018.02.009>.
- Lal, D., 1991. Cosmic ray labeling of erosion surfaces: in situ nuclide production rates and erosion models. *Earth and Planetary Science Letters*, 104(2-4), pp.424-439.
- Lague, D., 2014. The stream power river incision model: evidence, theory and beyond. *Earth Surface Processes and Landforms*, 39(1), pp.38-61.
- Nishiizumi, K., 2004. Preparation of ^{26}Al AMS standards. *Nuclear Instruments and Methods in Physics Research Section B: Beam Interactions with Materials and Atoms*, 223, pp.388-392.
- Nishiizumi, K., Imamura, M., Caffee, M.W., Southon, J.R., Finkel, R.C., and McAninch, J., 2007, Absolute calibration of ^{10}Be AMS standards: *Nuclear Inst. and Methods in Physics Research, B*, v. 258, no. 2, p. 403-413.
- Schaller, M., Ehlers, T.A., Stor, T., Torrent, J., Lobato, L., Christl, M. and Vockenhuber, C., 2016. Timing of European fluvial terrace formation and incision rates constrained by cosmogenic nuclide dating. *Earth and Planetary Science Letters*, 451, pp.221-231.
- Schildgen, T.F., Phillips, W.M. and Purves, R.S., 2005. Simulation of snow shielding corrections for cosmogenic nuclide surface exposure studies. *Geomorphology*, 64(1-2), pp.67-85.
- Stock, J.D. and Montgomery, D.R., 1999. Geologic constraints on bedrock river incision using the stream power law. *Journal of Geophysical Research: Solid Earth*, 104(B3), pp.4983-4993.
- Stone, J.O., 2000. Air pressure and cosmogenic isotope production. *Journal of Geophysical Research: Solid Earth*, 105(B10), pp.23753-23759.
- Wobus, C., Whipple, K.X., Kirby, E., Snyder, N., Johnson, J., Spyropoulos, K., Crosby, B., Sheehan, D., and Willett, S.D., 2006, Tectonics from topography: Procedures, promise, and pitfalls: *Geological Society of America Special Paper*, v. 398, p. 55, 10.1130/2006.2398(04).

Mahon, K.I., 1996. The New "York" regression: Application of an improved statistical method to geochemistry. International Geology Review, 38(4), pp.293-303.